Applied Mathematics and Mechanics
(English Edition, Vol 22, No 8, Aug 2001)

Published by Shanghai University,
Shanghai, China

Article ID: 0253-4827(2001)08-0904-13

EFFECTS OF SURFACE WAVES AND MARINE SOIL PARAMETERS ON SEABED STABILITY *

LIN Mian (林 缅), LI Jia-chun (李家春)

(Institute of Mechanics, CAS, Beijing 100080, P R China)

(Paper from LI Jia-chun, Member of Editorial Committee, AMM)

Abstract: *Based on the Yamamoto's soil model by considering the Coulomb friction effects, the wave-induced seabed instability has been investigated. An analytical solution is derived for soil response of a finite depth seabed under surface water wave. The effects of wave parameters and soil characteristics on the seabed instability are addressed for three types of soil. Finally, the roles of Coulomb friction stability are then analyzed as well.*

Key words: seabed instability; shear failure; liquefaction

CLC number: P731.2 **Document code**: A

Introduction

The most important forces exerting on coastal structures, such as offshore drilling rigs, offshore oil storage tanks, buried pipelines, breakwaters, etc. are due to water surface waves. The water waves propagating over the ocean can create tremendous dynamic pressure. The pressure transferred to the foundation directly or through structure leads to seabed deformation and results in instability. It was reported that some accidents of breakwaters are attributed to foundation failure rather than structural collapse[1,2]. As we know, marine soil consists of fine mineral particles and is suffered from enormous external force induced by gravity and storm. There is a periodical pressure on the interface of seabed and then transferred to porous seabed. According to the theory of elastic mechanics, the direction of principal stresses at a point within the marine soil is rotating continuously through 180° during one period of cyclic loading, but deviator stresses remain unchanged all the time and at all points on the horizontal plane during the interval. Such state should lead to the shear resistance reduction and seabed instability, including shear failure and liquefaction. The former occurs when the stress exceeds its shear resistance, while the latter is due to that pore pressure balances soil weight so that its particles in suspended state flows like a fluid.

Generally speaking, the study of seabed stability can be simplified as study of forced state of natural seabed. A number of theories for the wave-induced pore pressure have been proposed since early 1940s based on various assumptions regarding the physical properties of soil skeletal

* **Received date**: 2000-02-22; **Revised date**: 2001-03-06

Foundation item: the National Natural Science Foundation of China (19602021)

Biography: LIN Mian (1966 -), Associate Professor, Doctor

frame and pore fluid, such as rigidity, permeability, anisotropy, compressibility and degree of saturation. They can be separated into three kinds of models. Of these, the first model is for a rigid seabed with incompressible pore fluid (Putnam, 1949[3]; Sleath, 1970[4]; LIU, 1973[5]; Massel, 1976[6]; et al.); the second model is for a rigid seabed with compressible pore fluid (Moshagen, 1975[7]; Prevost, 1975[8]; et al.); and the third model is for an elastic porous medium with compressible pore fluid (Yamamoto, 1978[9]; Madsen, 1978[10]; Okusa, 1985[11]; et al.). The former two models have not been taken into account the coupling of pore-fluid motion and soil motion, which is governed by the Laplace equation of pore pressure (for the case of incompressible pore fluid) or the diffusion equation of pore pressure (for the case of compressible pore fluid). Such solutions for pore pressure are limited to particular cases of soil and wave condition, i.e., the Laplace equation for very permeable beds such as coarse sand beds, and the diffusion equation for very rigid and poorly permeable beds. And both models are unable to provide any information on stresses within the seabed. The third model is based on the Biot's theory of poro-elastic media and may be closest to the properties of marine soil. In recent years, such model has been applied to the study of breakwater failure. (Hus, 1994[12]; Semour, 1996[13]; Lin, 1996, 1997[14,15]; Jeng, 1997[16]; et al.). However, the internal frictions of soil have not been considered yet by this approach. As compared to the seepage force and elastic force, the inertia force of soil and fluid are negligibly small. This is equivalent to the assumption that the elastic wave speeds in a skeletal frame are infinitely large as compared to water surface wave speed. The assumption is reasonable for relatively rigid beds such as sand beds. Some experiment[17] results have found that the shear modulus are functions of shearing strain amplitude, magnitude of confining pressure, duration of confinement and number of cycles of loading, but nearly independent of loading frequency. So it should suggest that the shear energy dissipation come from the Coulomb friction, but not viscous damping or fluid-solid friction. Particularly, the effects of Coulomb friction are more significant within the fine sand or silt bed than coarse sand bed. Therefore, it is not only to treat the soil as pore-elastic media, but also assume that the Coulomb friction or solid-solid friction in fine sand or silt seabed is not negligible. In this paper, a general solution, by using Yamamoto's Coulomb-damping poroelastic model[18] for a finite seabed proposed by LIN (1999)[19] is employed to further investigate the wave-induced seabed instability. Based on the present model together with the criteria of liquefaction and shear failure, the wave-induced liquefaction and shear failure can then be estimated. The effects on instability of seabed including two types of fine sand bed and a coarse sand bed are discussed for various factors, such as wave steepness, relative water depth, period, relative seabed thickness, soil permeability and degree of saturation. Comparing the present results with Jeng's numerical one, we find that the influences of soil Coulomb friction on seabed instability are apparent at least for fine soil.

1 Theoretical Model

When considering the interaction of water waves with seabed, the analysis of soil response to external forcing is based on the following two basic assumptions:

1) The ocean water above depth $z = 0$ is assumed to be incompressible and inviscid and its motion is irrotational. Thus, the velocity potentials satisfy the Laplace's equation and the general

solution of potential function φ is readily found in the following form:

$$\varphi = \mathrm{i}a_0 g\{\cosh[\tilde{k}(z-h)]/\omega + \omega\sinh[\tilde{k}(z-h)]/g\tilde{k}\}\mathrm{e}^{\mathrm{i}(\omega t-\tilde{k}x)},$$

where a_0 is the wave amplitude at $x = 0$; h, the water depth; g, the gravitational constant; $\tilde{k}$, the complex wave number. Theory developed herein is for linear water wave propagation over elastic seabed.

2) The seabed is regarded as homogeneous poro-elastic medium. The total stresses in porous media under a plane strain condition are given as

$$\tau_{xx} = \tilde{H}e - 2\tilde{\mu}e_z - \tilde{C}\zeta,\ \tau_{zz} = \tilde{H}e - 2\tilde{\mu}e_x - \tilde{C}\zeta,\ \tau_{xz} = \tilde{\mu}\gamma,\ p = \tilde{M}\zeta - \tilde{C}e, \tag{1}$$

where τ_{xx}, τ_{zz}, τ_{xz} are the total stress components of the bulk material; and p is the pore pressure; the variable ζ is defined as: $\zeta = -\nabla \boldsymbol{w}$, where $\boldsymbol{w} = \beta(\boldsymbol{U} - \boldsymbol{u})$, $\boldsymbol{U}$ is the displacement of the pore fluid and β is the porosity of the soil; $\tilde{H}$, $\tilde{\mu}$, $\tilde{C}$, $\tilde{M}$ denote Biot's elastic moduli of porous media respectively and are complex constants due to the slightly inelastic nature of the soil. The complex moduli are the linearized expression of nonlinear Coulomb damping due to the grain-to-grain friction and energy dissipated due to the viscosity. The strain components of the skeletal frame of soil are $e = (e_x + e_z)$, $e_x(= \partial u_x/\partial x)$, $e_z(= \partial u_z/\partial z)$, $\gamma = (\partial u_z/\partial x + \partial u_x/\partial z)$, where u_x, u_z are the components of the displacement vector $\boldsymbol{u}$. In the next section, the constitutive equation will be adopted.

The proposed model of wave-soil interactions is based on the assumption of compressible skeletal frame and pore fluid of seabed soil. The motion of the pore fluid relative to the skeletal frame is assumed to obey the Darcy's law. The momentum equations of marine soil frame and the pore water can be written as[20]:

$$\left.\begin{aligned} &\frac{\partial^2}{\partial t^2}(\rho\boldsymbol{u} + \rho_f\boldsymbol{w}) = \tilde{\mu}\nabla^2\boldsymbol{u} + (\tilde{H} - \tilde{\mu})\nabla e - \tilde{C}\nabla\zeta, \\ &\frac{\partial^2}{\partial t^2}(\rho_f\boldsymbol{u} + m\boldsymbol{w}) + \frac{\eta_f}{k_s}\frac{\partial \boldsymbol{w}}{\partial t} = \nabla(\tilde{C}e - \tilde{M}\zeta), \end{aligned}\right\} \tag{2}$$

where k_s is the hydraulic coefficient of soil permeability; η_f is the viscosity of pore fluid; ρ_r and ρ_f are densities of grain and fluid, respectively; and $\rho = (1-\beta)\rho_r + \beta\rho_f$ is the bulk density of soil; the quantity $m = (\rho_f/\beta)(1+\alpha)$ is the reduced mass including added mass effects of soil skeletal frame in terms of added mass coefficient α.

Because skeletal frame has both rigidity and compressibility, two kinds of stress waves: shear waves and compressible waves, transmit though the skeletal frame. And there is another compressible wave through the pore fluid because of its compressibility. As a matter of fact, compression of pore fluid flow and deformation of skeletal frame take place simultaneously. Thus we have defined the three kinds of elastic waves propagating in the seabed. The first elastic waves are the fast compressible waves in which the pore water and the solid skeletal frame move together. The second elastic waves are the slow compressible waves that result from seepage motion of pore water relative to the moving soil skeletal frame. The last waves are shear waves. We have noticed that Eq.(2) is linear, therefore, each time-independent term of displacement vectors of solid and fluid can be represented by the sum of two longitudinal waves and the transverse wave:

$$\begin{cases} \boldsymbol{u} = \nabla\phi_f + \nabla\phi_s + \nabla\times\phi_T\hat{e}_y, \\ \boldsymbol{w} = \nabla\psi_f + \nabla\psi_s + \nabla\times\psi_T\hat{e}_y. \end{cases} \tag{3}$$

Furthermore, assumption of harmonic of loading waves in time and x-direction, the $\phi_{f,s,T}$, $\psi_{f,s,T}$ can be expressed in terms of to $e^{i(\omega t-\tilde{k}x)}$. Putting $\psi_{f,s,T} = \tilde{c}_{f,s,T}\phi_{f,s,T}$, and substituting it into Eq.(2), we have

$$\nabla^2\phi_{f,s,T} + k^2_{f,s,T}\phi_{f,s,T} = 0, \tag{4}$$

with

$$\left.\begin{aligned} &\tilde{k}_f^2 + \tilde{k}_s^2 = \frac{\omega^2(\tilde{H}\tilde{m} + \rho\tilde{M} - 2\rho_f\tilde{C})}{\tilde{H}\tilde{M} - \tilde{C}^2}, \\ &\tilde{k}_f^2\tilde{k}_s^2 = \frac{\omega^4(\tilde{m}\rho + \rho_f^2)}{\tilde{H}\tilde{M} - \tilde{C}^2}, \quad \tilde{k}_T^2 = \frac{\omega^2(\rho - \rho_f^2/\tilde{m})}{\tilde{\mu}}, \end{aligned}\right\} \tag{5}$$

and

$$\tilde{c}_{f,s} = -\frac{\tilde{H} - \tilde{V}_{f,s}\rho}{\tilde{C} - \tilde{V}_{f,s}\rho_f}, \quad \tilde{c}_T = -\frac{\rho_f}{\tilde{m}}.$$

From the above equations, we define the wave velocity of the three elastic waves:

$$\tilde{V}_{f,s,T} = \omega/\tilde{k}_{f,s,T}.$$

The general solution of Eq.(4) for harmonic in both time and x-direction is given by

$$\phi_{f,s,T} = [\tilde{a}_{1(f,s,T)}e^{\tilde{\lambda}_{f,s,T}Z} + \tilde{a}_{2(f,s,T)}e^{-\tilde{\lambda}_{f,s,T}Z}]e^{i(\omega t-\tilde{k}x)},$$

where $\tilde{\lambda}^2_{f,s,T} = \tilde{k}^2 - \tilde{k}^2_{f,s,T}$ and the six complex coefficient $\tilde{a}_{1,2(f,s,T)}$ and dispersion relation ($\tilde{k}$, ω) can be determined from the boundary conditions.

First of all, at the bed surface $z = 0$, they should meet the conditions at the interface between water and seabed. The boundary conditions are that the vertical effective stress is zero, that the shear stress is zero, that the fluid pressure is transmitted continuously from the sea to the pores in the seabed and that the mass of fluid must be conserved:

$$\tau_{zz} + p = 0, \ \tau_{xz} = 0, \ p = -\rho_f\partial\varphi/\partial t, \ \partial\varphi/\partial z = \partial u_z/\partial t + \partial w_z/\partial t.$$

Then assume that the bottom of seabed $z = -d$ is a rigid boundary, thus:

$$u_x = 0, \ u_z = 0, \ w_z = 0.$$

From the above seven equations, the six coefficients $\tilde{a}_{1(f,s,T)}$, $\tilde{a}_{2(f,s,T)}$ and the dispersion relation turn out[19]:

$$\tanh(\tilde{k}h) = \frac{\omega^2}{g\tilde{k}}\left[1 - \frac{w_z(0) + u_z(0)}{a_0\cosh\tilde{k}h}\right]. \tag{6}$$

So the pore pressure and the total stress components are given as

$$\begin{aligned} p = {} & \{(\tilde{a}_{1f}e^{\tilde{\lambda}_f Z} + \tilde{a}_{2f}e^{-\tilde{\lambda}_f Z})[\tilde{C} + \tilde{c}_f\tilde{M}]\tilde{k}_f^2 + \\ & (\tilde{a}_{1s}e^{\tilde{\lambda}_s Z} + \tilde{a}_{2s}e^{-\tilde{\lambda}_s Z})[\tilde{C} + \tilde{c}_s\tilde{M}]\tilde{k}_s^2\}e^{i(\omega t-\tilde{k}x)}, \\ \tau_{xx} = {} & \{(-\tilde{a}_{1f}e^{\tilde{\lambda}_f Z} - \tilde{a}_{2f}e^{-\tilde{\lambda}_f Z})[(\tilde{H} + \tilde{c}_f\tilde{C})\tilde{k}_f^2 + 2\tilde{\mu}\tilde{\lambda}_f^2] + \\ & (-\tilde{a}_{1s}e^{\tilde{\lambda}_s Z} - \tilde{a}_{2s}e^{-\tilde{\lambda}_s Z})[(\tilde{H} + \tilde{c}_s\tilde{C})\tilde{k}_s^2 + 2\tilde{\mu}\tilde{\lambda}_s^2] + \\ & (\tilde{a}_{1T}e^{\tilde{\lambda}_T Z} - \tilde{a}_{2T}e^{-\tilde{\lambda}_T Z})2i\tilde{\mu}\tilde{k}\tilde{\lambda}_T\}e^{i(\omega t-\tilde{k}x)}, \\ \tau_{zz} = {} & \{(-\tilde{a}_{1f}e^{\tilde{\lambda}_f Z} - \tilde{a}_{2f}e^{-\tilde{\lambda}_f Z})[(\tilde{H} + \tilde{c}_f\tilde{C})\tilde{k}_f^2 - 2\tilde{\mu}\tilde{k}^2] + \\ & (-\tilde{a}_{1s}e^{\tilde{\lambda}_s Z} - \tilde{a}_{2s}e^{-\tilde{\lambda}_s Z})[(\tilde{H} + \tilde{c}_s\tilde{C})\tilde{k}_s^2 - 2\tilde{\mu}\tilde{k}^2] + \\ & (\tilde{a}_{1T}e^{\tilde{\lambda}_T Z} + \tilde{a}_{2T}e^{-\tilde{\lambda}_T Z})2i\tilde{\mu}\tilde{k}\tilde{\lambda}_T\}e^{i(\omega t-\tilde{k}x)}, \\ \tau_{xz} = {} & \{(-\tilde{a}_{1f}e^{\tilde{\lambda}_f Z} + \tilde{a}_{2f}e^{-\tilde{\lambda}_f Z})2i\tilde{\mu}\tilde{k}\tilde{\lambda}_f + (-\tilde{a}_{1s}e^{\tilde{\lambda}_s Z} + \tilde{a}_{2s}e^{-\tilde{\lambda}_s Z})2i\tilde{\mu}\tilde{k}\tilde{\lambda}_s + \end{aligned}$$

$$(\tilde{a}_{1T}e^{\tilde{\lambda}_T Z} - \tilde{a}_{2T}e^{-\tilde{\lambda}_T Z})(2\tilde{k}^2 - \tilde{k}_T^2)\tilde{\mu}\}e^{i(\omega t - \tilde{k}x)}.$$

The solutions for the wave-induced soil response given by above equations are applicable to the study of seabed instability in the next section.

2 Criteria of Seabed Instability[16]

2.1 Shear failure

When the shear stresses at a point in the marine soil are large enough to exceed its shear resistance, actual instability in seabed occurs. The real process of such failure will depend on the spatial distribution of wave-induced shear stress and the shear strength of the soil. Usually estimation of failure stresses for soils has been based on the Mohr-Coulomb criterion, which is still the most widely accepted in geotechnical practice so far. For now only the wave-induced incremental changes in stresses and pressures in soils from the initial equilibrium state have been considered. Later the total effective stress in z-direction, x-direction, and the total effective shear stress will be given. According to the traditional sign convention for stresses in the soil mechanics, i.e. a stress is positive when it acts as compression, the total effective stresses and shear stress are written by

$$\left.\begin{aligned} \bar{\tau}_{zz} &= \tau_{z0} - \tau'_{zz} = -(\gamma_r - \gamma_f)K_0 z - \tau_{zz} - p, \\ \bar{\tau}_{xx} &= \tau_{x0} - \tau'_{xx} = -(\gamma_r - \gamma_f)z - \tau_{xx} - p, \\ \bar{\tau}_{xz} &= -\tau'_{xz}, \end{aligned}\right\} \tag{7}$$

where τ_{z0}, τ_{x0} are the effective stresses at initial equilibrium in the z-direction and x-direction, respectively, γ_r, γ_f are the unit weight of soil and water; and the K_0 (its value for soil ranges from 0.4 to 10.) is the coefficient of earth pressure at rest and is related to the Poisson ratio, ν, as: $K_0 = \nu/(1-\nu)$; τ_{zz}, τ_{xx}, τ_{xz} can be obtained by Eq.(7). The effective principal stresses σ_1, σ_3 can be expressed in terms of $\bar{\tau}_{xx}$, $\bar{\tau}_{zz}$, $\bar{\tau}_{xz}$ as

$$\sigma_{1,3} = \frac{\bar{\tau}_{xx} + \bar{\tau}_{zz}}{2} \pm \sqrt{\left(\frac{\bar{\tau}_{xx} - \bar{\tau}_{zz}}{2}\right)^2 + \bar{\tau}_{xz}^2}.$$

The stress state at a specific location and instance may be conveniently expressed by the angle ϑ between the tangent from the origin to the instantaneous Mohr's circle and the σ-axis, which turns out the so-called stress angle given by

$$\sin\vartheta = \frac{\sigma_1 - \sigma_3}{\sigma_1 + \sigma_3} = \frac{\sqrt{(\bar{\tau}_{xx} - \bar{\tau}_{zz})^2 + 4\bar{\tau}_{xz}^2}}{(\bar{\tau}_{xx} + \bar{\tau}_{zz})}.$$

The failure condition for a given soil may be written as

$$\tau_f = \sigma_f \tan\vartheta_f.$$

where ϑ_f represents the angle of internal friction of soil and depends on the soil type, for example, 32° ~ 40° for sands and 28° ~ 36° for silt; τ_f and σ_f represent the effective shear stress and normal stresses on the failure plane, respectively. Then the failure criteria of the soil element at a given point and a given instance may be defined as

$$\vartheta(x,z,t) = \arcsin\left(\frac{\sqrt{(\bar{\tau}_{xx} - \bar{\tau}_{zz})^2 + 4\bar{\tau}_{xz}^2}}{(\bar{\tau}_{xx} + \bar{\tau}_{zz})}\right) \geqslant \vartheta_f. \tag{8}$$

2.2 Soil liquefaction

The wave-induced soil liquefaction in marine sediment is another form of soil breakdown

different from shear failure. Usually liquefaction is considered as a sort of quick sand boiling process. The dynamic stresses and strain due to periodical surface waves lead to volumetric compaction by granular slip. Consequently, the relaxation in soil skeleton generate effective stresses to the pore water, thus enhancing the pore-water pressure within the soil skeleton and reducing effective stresses. In the extreme case, the excess pore pressure may increase drastically to eliminate stresses in soil, and then sand flows and liquefaction occurs. Although the soil has lost the strength to carry any load as it is liquefied, the mechanism of liquefaction has not been clearly revealed thus far. The liquefaction is obviously affected by the state of soil compaction, permeability and the wave-induced cyclic stress, as well as the degree of drainage. Now we will only discuss the transient liquefaction. What is called transient liquefaction (i.e. infancy liquefaction) is instantaneous response of soil skeleton and pore water to loading waves. Theoretically, transient liquefaction may not affect the soil deformation later and is only regarded as a basis to estimate the soil behaviors. But if the liquefaction occurs near the bed surface, the repetitive nature of liquefaction over the large number of wave cycles may result in bed scouring sufficiently critical to cause significant damage to offshore structure. So the investigation of the soil transient liquefaction is necessary. Now three criteria of liquefaction have been suggested to define the liquefied state in a porous seabed. Among these are:

① Okusa[11] (1985) proposed that a soil skeleton would be liquefied when its effective vertical normal stress is greater than the submerged weight of soil deposits. i.e.

$$-(\gamma_r - \gamma_w)z - \sigma_z' \leqslant 0;$$

② Tsai (1995)[21] assumed that liquefaction occurs when its mean effective normal stress becomes zero. Thus the criterion of soil liquefaction based on the three-dimensional elastic analysis can be expressed as

$$\frac{1}{3}[-(\gamma_r - \gamma_w)(1 + 2K_0)z - (\sigma_x' + \sigma_y' + \sigma_z')] \leqslant 0;$$

③ Zen and Yamazaki (1990)[22] considered that at a point within the soil bed, the wave liquefaction in soil occurs when the submerged weight of a soil skeleton is less than the upward seepage force exerted on it. Later they extended the concept to a 2D condition. Such that:

$$-(\gamma_r - \gamma_w)z + (P_b - p) \leqslant 0.$$

Where $P_b - p$ is excess pore pressure (it is also called the excess hydrostatic pressure). P_b is the water pressure on the seabed surface varies according to the propagation of waves, p is the wave-induced pore pressure within soils. The positive or negative of the excess pore pressure implies the pore water flow upward or downward. It is noted that this criterion is based on the assumption of ratio of seabed thickness and wave length being much smaller than 1 (i.e. $d/L < 1$).

All the criteria cited from above-mentioned[16] have applied oscillatory effective normal stress and pore pressure, thus neglecting the residual effect, since the knowledge of the later is immature. Based on the former equations of pore pressure and effective stresses, the complex elastic modulus $\tilde{M}$, $\tilde{C}$ is closely related to pore pressure, but the modulus $\tilde{\mu}$ to effective stresses. Thus the value σ_z' may be grossly in error when it approaches zero. Consequently, the liquefaction criteria ① and ② based on the effective normal stress would not be applicable. Thus the liquefaction criterion ③, employing the excess pore pressure, may be the only meaningful condition. In the next section we will apply criterion ③ to the analysis of seabed liquefaction.

3 Results and Analysis

In this section, we plan to investigate the dependence of soil response to external cyclic loading due to surface waves for six groups of parameters based on the formulas given in Section 2:

a) Wave height: In practical engineering applications, wave height has been commonly expressed in terms of wave steepness, A/L, which is the ratio of wave height to wave length and ranges from 0.025 to 0.125;

b) Relative depth: The relative water depth H/L, which has been recognized by coastal engineers as a dominant factor of wave characteristics. The wave field is considered as in a shallow water when $H/L < 0.10$, as in deep water when $H/L > 0.5$. In this example, the relative water depth is considered from 0.10 for shallow water to 0.5 for deep water;

c) Wave period: T, it ranges from 10s to 20s;

d) Seabed thickness: The values of relative seabed thickness d/L vary from 0.05 to 0.7, which covers the possible rang of seabed thickness in practical engineering applications;

e) Permeability: This is a parameter to characterize the ability of seabed drainage. We select values from 10^{-5} m/s to 10^{-2} m/s;

f) The degree of saturation: its value ranges from 0.95 to 1.0.

Three types of non-cohesive soil have been examined here. The soil parameters have been listed in Table 1. It is noted that the soil properties are the common parameters for marine sediments and the fine sand 2 is softer than fine sand 1 and more similar to cohesive soil.

Table 1 The calculated parameters

parameters		soil	fine sand-1	fine sand-2	coarse sand
wave steepness (A/L)	0.025 ~ 0.125	porosity β	0.3	0.33	0.3
relative water depth (H/L)	0.1 ~ 0.5	Poisson's ratio ν	0.33	0.33	0.33
wave period T/s	10 ~ 20	shear modulus G/N/m^2	10^7	10^6	5×10^7
seabed thickness (d/L)	0.05 ~ 0.7	permeability k_s/m/s	10^{-4}	10^{-5}	10^{-2}
permeability k_s/m/s	10^{-5} ~ 10^{-2}	pore fluid viscosity η_f/kg/ms	10^{-3}	10^{-3}	10^{-3}
degree of saturation S_r	0.95 ~ 1.0	unit weight of soil /unit weight of water γ_r/γ_f	2	2	2

Based on the general solutions together with the criteria of liquefaction and shear failure, we examine the influences of wave and soil characteristic on the wave-induced seabed instability. To begin with, it is necessary to know the maximum liquefaction depth and maximum shear failure depth within one wavelength. The curves of liquefaction depth and shear failure depth are illustrated in Fig.1 for a saturated fine sand seabed. It is clearly shown that the maximum shear failure is located under the wave crest, whereas the maximum liquefaction depth is located under the wave trough. And the maximum liquefaction depth is 3 times of maximum shear failure depth. That is to say it is easier for shear failure or scour to happen near seabed surface and the

phenomenon of liquefaction occurs in deep seabed. Then we will separately take the values of liquefaction depth at the wave crest and shear failure depth under the wave trough as reference points for the seabed instability study.

The calculated values are plotted vs. wave steepness in Fig.2(a). As shown in the figure, the maximum depth of liquefaction decreases with the wave steepness for fine sand. To coarse sand, when the wave period is 12.5s, water depth 40m, wave steepness less than 0.12, no liquefaction occurs. However, when wave steepness is greater than 0.12, the depths of shear failure grows rapidly, as $A/L > 0.145$, the failed depth for coarse sand bed will even be in excess of the depth for fine sand. This can be understood in physics because small waves can not affect such seabed. Again, the maximum depth of shear failure is larger for coarse sand than that for fine sand. As $A/L \sim 0.083$, the depth z/d reaches 0.7. On the contrary, the depths for fine sand are the same as wave steepness increases. So both liquefaction and shear failure for coarse sand should be paid more attention to large wave steepness situations.

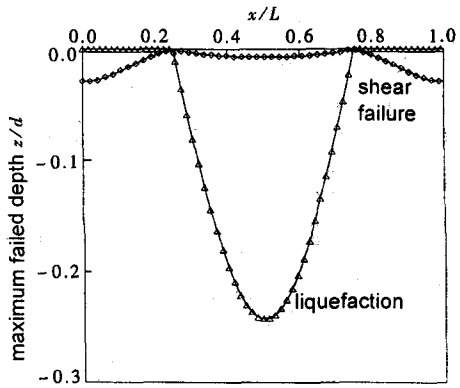

Fig.1 The distribution of maximum failed depth within a wavelength

Similar trends can also be observed in Fig.2(b), the maximum depths of liquefaction decreases with the relative water depth. It may be concluded that waves in shallow water may be able to cause a larger failure than that in deep water. When $H/L > 0.26$, wave height 5m and wave period 12.5s, no liquefaction occurs for fine sand-1, but there is liquefied phenomenon within the fine sand-2. At the same wave condition, no liquefaction happens at any relative water depth for coarse sand. According to the distribution of maximum failure depth due to shear failure, we know that the failure depth decreases as relative water depth increases for coarse sand, and the failed depth is not only rather shallow but also no variation with the relative water depth for fine sand-2. The situation for fine sand-1 is more complex. At first the depth increases as water depth increases, and reaches the maximum value at $H/L = 0.22$ and decreases thereafter. For the loading wave example presented now, the seabed is stable as $H/L > 0.35$; when $H/L < 0.35$, the breakdown is mainly due to shear for coarse sand and due to liquefaction for fine sand-2; both causes should be considered for fine sand-1, especially as $H/L \sim 0.22$.

We have computed the failure depth vs. wave periods for fine and coarse sands (Fig.2(c) and Fig.3(c)). Fig.2(c) shows that the maximum liquefaction depth increases for fine sand as the wave period increases. Under the same wave height and water depth, a longer period may cause a larger liquefaction potential than a wave with a shorter period for fine sand, but there is almost no liquefaction for coarse sand. Fig.3(c) is the distribution of maximum shear failure depth vs. the wave periods. As the Fig.3(c) shows, the curve of the fine sand-1 is not monotonous. As $T = 10.5$s, the depth of shear failure reaches maximum, then it decreases as period increases and stabilizes at $z/d = 0.007$ when T > 14s. However, the curves of the fine sand-2 and coarse sand do not varied with various values of wave period. It is noted that the

failure depth for fine sand-1 is greater than that for other case and the principal failure is liquefaction for fine sand-2 and the shear failure for coarse sand.

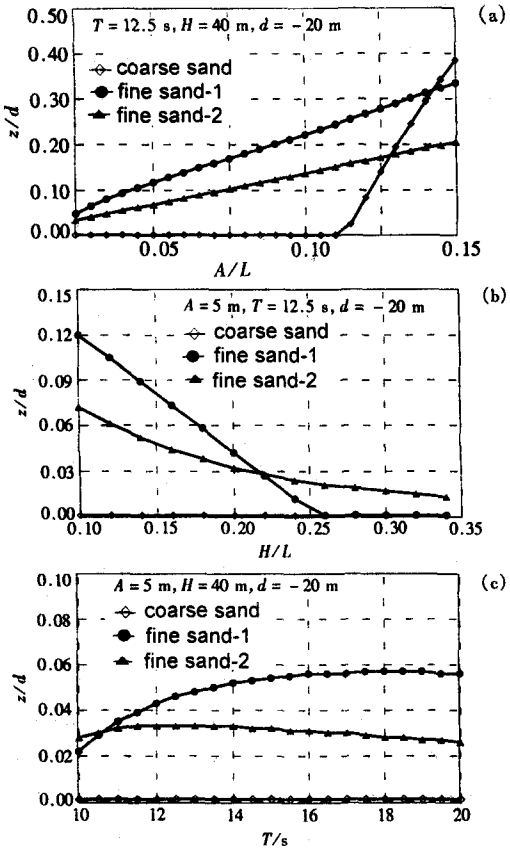

(a) wave steepness A/L
(b) relative water depth H/L
(c) wave period

Fig.2 Maximum liquefction depth (S_r = 0.98) vs

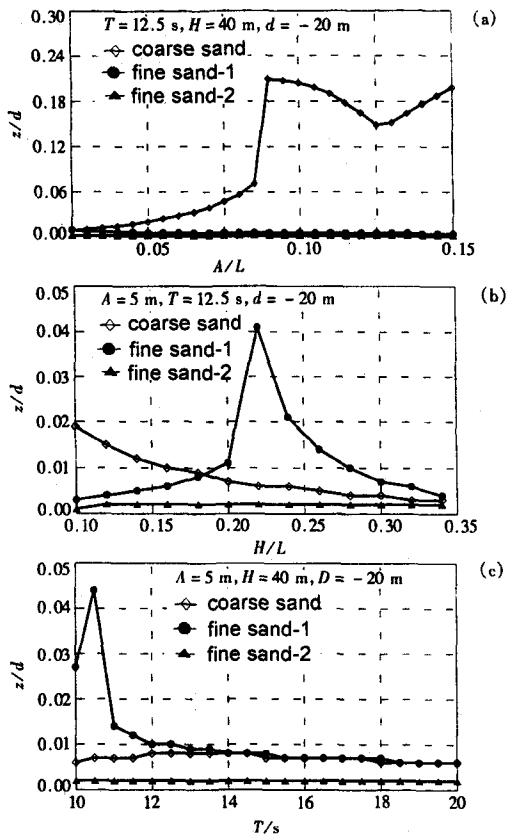

(a) wave steepness A/L
(b) relative water depth H/L
(c) wave period

Fig.3 Maximum shear failure depth (S_r = 0.98) vs

The maximum failure depths owing to liquefaction and shear failure are plotted in Fig.4 (a) and Fig.5 (a) vs. seabed thickness separately. As seen in Fig.4 (a), in the fine sand-1 and sand-2 seabed, the liquefaction depths decrease as d/L increases, and reach zero at $d/L = 0.41$ and $d/L = 0.37$ separately. In the coarse sand bed, the curve is almost a horizontal line and approaches zero. However, the depth of shear failure is not monotonous in the fine sand-1 seabed (Fig.5 (a)). The shear failure depth induced by water wave over fine sand-1 bed has a peak at $d/L = 0.27$. This implies that the most unstable bed exists when $d/L = 0.27$ because of the combined effect of incident elastic waves and reflected elastic waves by bedrock. Yamamoto[23] also found that there was an unstable seabed as $d/L = 0.2$ when he studied the sediments in the North Sea. Therefore, such susceptible region should be avoided in the design of ocean structures.

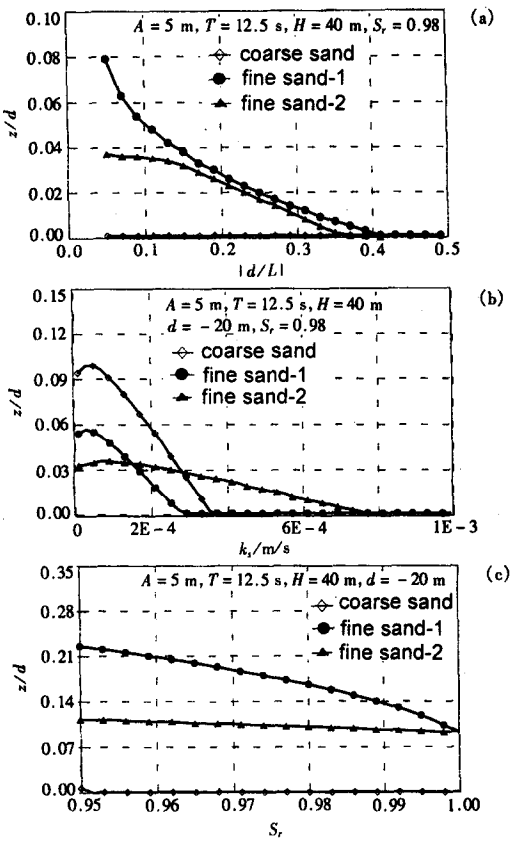

(a) relative seabed thickness d/L

(b) permeabilities k_s

(c) degree of saturation S_r

Fig.4 Maximum liquefaction depth vs

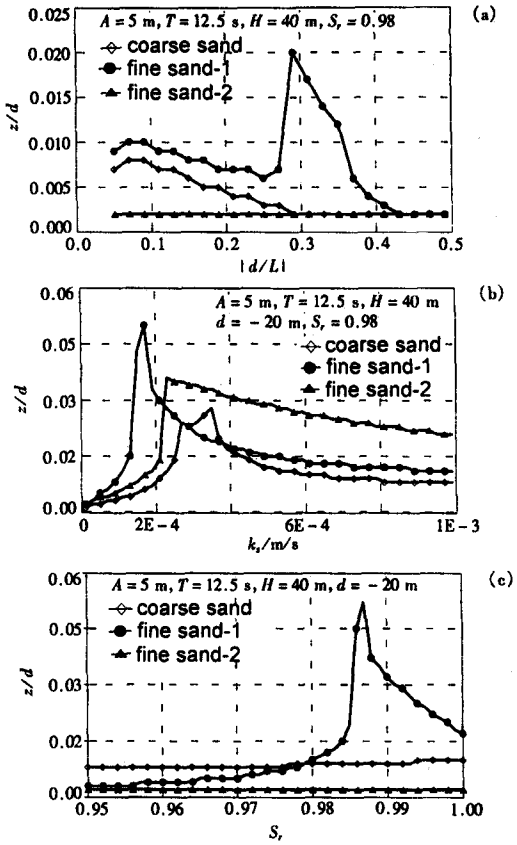

(a) relative seabed thickness d/L

(b) permeabilities k_s

(c) degree of saturation S_r

Fig.5 Maximum shear failure depth vs

Fig.4 (b) and Fig.5 (b) illustrate the distribution of the maximum failure depth due to liquefaction and shear failure vs. permeability. It is obvious that the liquefaction depth and shear failure depth reach limit at some permeability. For example, when $T = 12.5$ s, $H = 40$ m, $A = 5$ m, as k_s is about $10^{-5} \sim 2.5 \times 10^{-4}$ m/s, liquefaction always happens; $k_s > 3.5 \times 10^{-4}$ m/s, the liquefaction only occurs in fine sand-2; $k_s > 8 \times 10^{-4}$m/s, no liquefaction occurs. This is because that the pore fluid drains away easily in that case. The failure depth due to shear is significant for permeability 10^{-4}m/s $< k_s 4 \times 10^{-4}$ m/s. As $k_s > 4. \times 10^{-4}$ m/s, the depth of shear failure almost does not vary with the permeability. This implies that the shear failure is susceptible in a seabed with the permeability around 10^{-4}m/s.

The soil response is affected considerably by the degree of saturation. As in the examples presented, the degree of saturation is considered to vary from 0.95 to 1.0 (Fig.4 (c) and Fig.5 (c)). Generally speaking, the maximum liquefaction decreases as the saturation increases. The liquefaction depth for fine sand-1 and fine sand-2 approaches the same as $S_r = 1.0$. The values for fine sand-2 and coarse sand vary slowly with the degree of saturation and similar cases can be

found in the failed owing to shear failure. However, the maximum failed depth due to shear is different over the fine sand-1 bed. The distribution of failed depth vs. saturation gets a top at $S_r = 0.985$ and then is reduced rapidly. It is can be concluded that the more saturation a seabed is, the more stable seabed becomes. But it is not valid for fine sand-1. We will discuss the problem further.

As compared with above figures, the influence of coarse sand on the wave-induced liquefaction and shear failure is almost linear. This is because that the fast shear wave speed and shear waves speed is much greater than water wave speed and the pressure on the bottom surface is hardly affected by the motion of seabed. However response of fine sand, especially for fine sand-1, is more complex. In order to understand the properties of fine sand, we study the problem further more and compare our numerical results with Jeng (1997)'s, who applied poroelastic model for soil (that is the third model mentioned above).

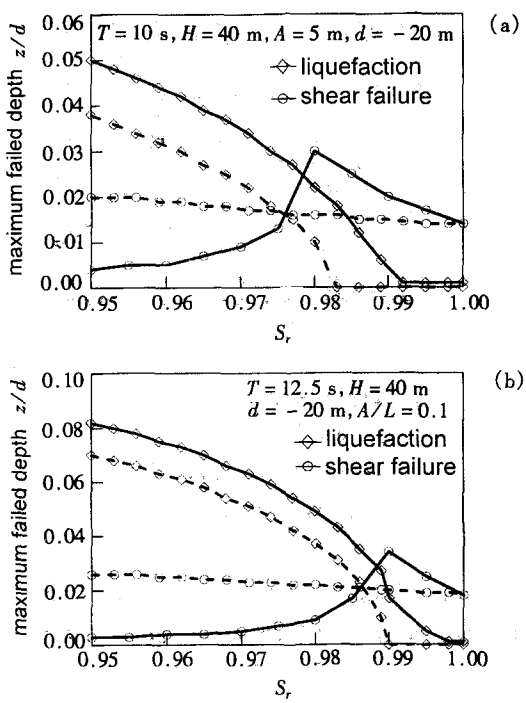

—Authors, ---Jeng (1997)

(a) $T = 10s$ (b) $A/L = 0.1$

Fig.6 Distribution of the maximum failed depth vs the degree of saturation S_r

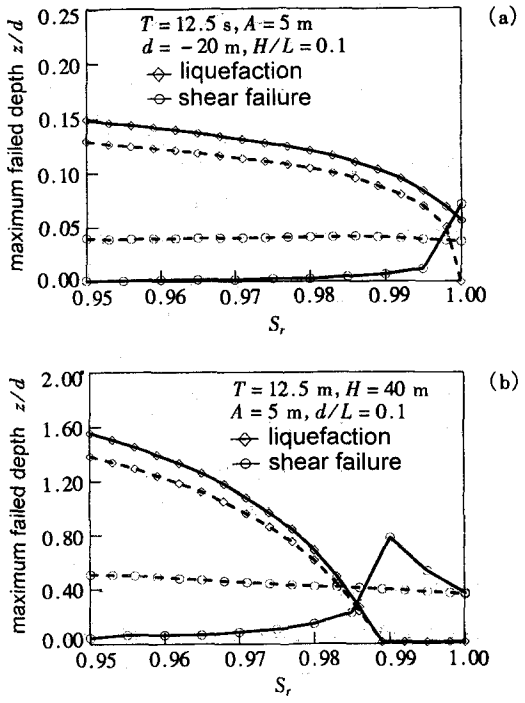

—Authors, ---Jeng (1997)

(a) $H/L = 0.1$ (b) $d/L = 0.1$

Fig.7 Distribution of the maximum failed depth vs the degree of saturation S_r

As shown in Fig.6 and Fig.7, the distribution of non-dimensional maximum failure depth for liquefaction or shear failure, z/d, vs. the degree of saturation S_r is presented for fine sand-1 (Jeng's numerical results are plotted with dash lines). Generally speaking, the liquefaction depth decreases as the degree of saturation increases and similar trends can be observed in dash line. The difference of both curves is because the Jeng's results are for breakwaters. But, in the shear failure case, the curves are different entirely. As shown in these figures, the depth of shear failed

increases as the degree of saturation increase during low degree of saturation. When S_r is between the range of 0.98 ~ 0.99, there exist peak values in different cases. But the Jeng's results show that the depth of shear failure almost remains unvaried with different degrees of saturation and appears horizontal. The conclusion is similar to our results for coarse sand (see Fig.5 (c)). That is to say, viewing from other angle the poroelastic model is appropriate for coarse sand. In the fine sand bed, when the speed of shear wave approaches the speed of water wave, the resonance may occur and the shear vibration becomes considerably amplified. However, meanwhile, the internal damping of seabed soil becomes large enough to suppress the resonance vibration. So we have estabished that the peaks are attributed to the interaction of resonance and Coulomb friction. In the fine sand-2 bed, because the loading waves is too small to induce shear failure based on the examples presented in this study, no similar phenomena occur in the bed. On the other hand, because the criteria of liquefaction used in the paper are only related to the pore pressure, but not to shear stress, the effect of Coulomb friction doesn't manifest itself.

4 Conclusions

In this paper, the wave-induced seabed instability for three types of soil is treated based on the Yamamoto's coulomb-damping pore elastic model. The influences of the six group parameters on the seabed response to surface wave loading have been examined. The results can be summarized as follows:

Fine sand-1: Generally speaking, both failure due to liquefaction and shear stress is important and the effects of all parameters on the maximum failure depth are rather obvious, especially on shear failure. Because of the Coulomb friction, the failure depth due to shear stress reaches extreme in some special ranges. Based on the case studies presented in the article, the following critical parameters range should be paid more attention to: ① Water wave period around 10s; ② Water depth $H/L \sim 0.22$; ③ Seabed thickness $d/L \sim 0.3$; ④ Permeability $k_s \sim 1.4 \times 10^{-4}$; ⑤ Degree of saturation $0.975 < S_r < 0.985$.

Fine sand-2: The soil is softer than fine sand-1. In general cases, the failure due to liquefaction often takes place in comparison with the failure due to shear failure.

Coarse sand: The failure due to shear stress is more serious than that due to liquefaction, especially in storms. As in the example presented in the paper, the seabed is unstable as $A/L > 0.08$ and permeability $k_s \approx 2 \times 10^{-4} \sim 4 \times 10^{-4}$ m/s.

References:

[1] Smith A W, Gordon A D. Large breakwater toe failures [J]. *Journal of Waterway Port Coastal and Ocean Engineering*, *A S C E*, 1983, **109**(2):253 - 255.

[2] Silvester R, Hsu J R C. Sines revisited [J]. *Journal of Waterway Port Coastal and Ocean Engineering*, *A S C E*, 1989, **115**(3):327 - 344.

[3] Putnam J A. Loss of wave energy due to percolation in a permeable sea bottom [J]. *Trans Am Geophys Un*, 1949, **30**:662 - 666.

[4] Sleath J F A. Wave induced pressures in beds of sand [J]. *J Hydraul Div A S C E*, 1970, **96** (HY2):367 - 378.

[5] Liu P L-F. Damping of waves over porous bed [J]. *J Hydraul Div A S C E*, 1973, **99**(HY12): 2263 - 2271.

[6] Massel S R. Gravity waves propagated over permeable bottom [J]. *J Watways Harb Cstl Engng A S C E*, 1976, **102**(WW2): 111 - 121.

[7] Moshagen H, Torum A. Wave induced pressures in permeable seabed [J]. *J Watways Harb Cstl Engng A S C E*, 1975, **101**(WW1): 49 - 58.

[8] Prevost J H, Eide O, Anderson K H. Discussion of wave induced pressure in permeable seabed [J]. *J Watways Harb Cstl Engng A S C E*, 1975, **101**(WW4): 464 - 465.

[9] Yamamoto T, Koning H L, Sellmeijer H, et al. On the response of a poro-elastic bed to water waves [J]. *Journal Fluid Mechanics*, 1978, **87**(1): 193 - 206.

[10] Madsen O S. Wave-induced pore pressures and effective stresses [J]. *Geotechnique*, 1978, **28**(4): 377 - 393.

[11] Oksua S. Wave-induced stresses in unsaturated submarine sediments [J]. *Geotechnique*, 1985, **35**(4): 517 - 532.

[12] Hus J R C, Jeng D S. Wave-induced soil response in an unsaturated anisotropic seabed of finite thickness [J]. *International Journal for Numerical and Analytical Methods in Geomechanics*, 1994, **18**: 785 - 807.

[13] Seymour B R, Jeng D S, Hus J R C. Transient soil response in porous seabed with a variable permeability [J]. *Ocean Engineering*, 1996, **23**(1): 27 - 46.

[14] Lin Y S, Jeng D S. Response of poro-elastic seabed to a 3-D wave system: a finite element analysis [J]. *Coastal Engineering in Japan*, 1996, **39**(2): 165 - 183.

[15] Lin Y S, Jeng D S. The effects of variable permeability on the wave-induced seabed response [J]. *Ocean Egineering*, 1997, **24**(7): 623 - 643.

[16] Jeng D S. Wave-induced seabed instability in front of a breakwater [J]. *Ocean Engng*, 1997, **24**(10): 887 - 917.

[17] Stokoe K H. Dynamic properties of offshore silty samples [A]. In: Program Departmen, Offshore Technology Conference Ed. *Offshore Technology Conference Proceedings* [C]. Richardson, T X 75083-3868, USA, 1980, **2**: 289 - 302.

[18] Yamamoto T. On the response of a Coulomb-damped poroelastic bed to water waves [J]. *Marine Geotechnology*, 1983, **5**(2): 93 - 127.

[19] LIN Mian. The analysis of silt behaviors induced by water waves [J] *Sci China Ser E*, 2000, **30**(6): 1 - 12. (in Chinese)

[20] Li J C, Lin M. On the interaction of water waves and seabed by porous mLedium model [J]. *Acta Mechanics Sinica*, 1995, **11**(2): 17 - 27.

[21] Tsai C P. Wave-induced liquefaction potential in a porous seabed in front of a breakwater [J]. *Ocean Engineering*, 1995, **22**(1): 1 - 18.

[22] Zen K, Yamazaki. Mechanism of wave-induced liquefaction and densification in seabed foundations [J]. *Soil and Foundations*, 1990, **30**: 90 - 104.

[23] Yamamoto T. Wave-induced pore pressures and effective stresses in inhomogeneous seabed foundations [J]. *Ocean Engng*, 1981, **8**: 1 - 16.